

Light Remodels Lipid Biosynthesis in *Nannochloropsis gaditana* by Modulating Carbon Partitioning between Organelles¹[OPEN]

Alessandro Alboresi², Giorgio Perin², Nicola Vitulo, Gianfranco Diretto, Maryse Block, Juliette Jouhet, Andrea Meneghesso, Giorgio Valle, Giovanni Giuliano, Eric Maréchal, and Tomas Morosinotto*

PAR-Lab_Padua Algae Research Laboratory, Department of Biology (A.A., G.P., A.M., T.M.), and Innovative Biotechnologies Interdepartmental Research Center (CRIBI; N.V., G.V.), University of Padova, 35121 Padova, Italy; Laboratoire de Biologie Cellulaire et Végétale, UMR 5168 CNRS, CEA, INRA, Université Grenoble Alpes, BIG, CEA-Grenoble, 38054 Grenoble, Cedex 9, France (M.B., J.J., E.M.); Department of Biotechnology, University of Verona, 37134 Verona, Italy (N.V.); and Italian National Agency for New Technologies, Energy, and Sustainable Economic Development (ENEA), Casaccia Research Centre, 00123 Roma, Italy (G.D., G.G.)

ORCID IDs: 0000-0003-4818-7778 (A.A.); 0000-0002-9204-4080 (G.P.); 0000-0002-0803-7591 (T.M.).

The seawater microalga *Nannochloropsis gaditana* is capable of accumulating a large fraction of reduced carbon as lipids. To clarify the molecular bases of this metabolic feature, we investigated light-driven lipid biosynthesis in *Nannochloropsis gaditana* cultures combining the analysis of photosynthetic functionality with transcriptomic, lipidomic and metabolomic approaches. Light-dependent alterations are observed in amino acid, isoprenoid, nucleic acid, and vitamin biosynthesis, suggesting a deep remodeling in the microalgal metabolism triggered by photoadaptation. In particular, high light intensity is shown to affect lipid biosynthesis, inducing the accumulation of diacylglyceryl-*N,N,N*-trimethylhomo-Ser and triacylglycerols, together with the up-regulation of genes involved in their biosynthesis. Chloroplast polar lipids are instead decreased. This situation correlates with the induction of genes coding for a putative cytosolic fatty acid synthase of type 1 (*FAS1*) and polyketide synthase (*PKS*) and the down-regulation of the chloroplast fatty acid synthase of type 2 (*FAS2*). Lipid accumulation is accompanied by the regulation of triose phosphate/inorganic phosphate transport across the chloroplast membranes, tuning the carbon metabolic allocation between cell compartments, favoring the cytoplasm, mitochondrion, and endoplasmic reticulum at the expense of the chloroplast. These results highlight the high flexibility of lipid biosynthesis in *N. gaditana* and lay the foundations for a hypothetical mechanism of regulation of primary carbon partitioning by controlling metabolite allocation at the subcellular level.

More than 45% of our planet's annual net primary biomass is obtained by the photosynthetic activity of microalgae that convert light energy into chemical

¹ A.A., G.P., A.M., and T.M. were supported by ERC starting grant BIOLEAP number 309485 to T.M. M.B., J.J., and E.M. were supported by grants from Agence Nationale de la Recherche (ANR DiaDomOil, ChloroMitoLipid, and Reglisse) and Infrastructure d'Avenir Océanomics. G.D. and G.G. were partially supported by Italian Ministry of Agriculture grant Hydrobio to G.G. The study benefited from the networking activities within the European Cooperation in Science and Technology Action CA15136 (EUROCAROTEN).

² These authors contributed equally to the article.

* Address correspondence to tomas.morosinotto@unipd.it.

The author responsible for distribution of materials integral to the findings presented in this article in accordance with the policy described in the Instructions for Authors (www.plantphysiol.org) is: Tomas Morosinotto (tomas.morosinotto@unipd.it).

T.M., G.G., and E.M. designed the research; A.A. and T.M. coordinated all experiments; G.P. and A.M. prepared biological material and performed physiological analysis; M.B., J.J., and E.M. performed lipidomic analysis and analyzed corresponding data; G.D. performed metabolomic analysis and analyzed corresponding data; N.V. and G.V. performed transcriptomic analysis and analyzed corresponding data; G.P. and A.A. analyzed and compared all data; A.A., G.P., T.M., E.M., and G.G. wrote the article.

[OPEN] Articles can be viewed without a subscription.

www.plantphysiol.org/cgi/doi/10.1104/pp.16.00599

energy in the chloroplast (Falkowski et al., 2004; Wang et al., 2011). The fixation of CO₂ within the Calvin-Benson cycle plays a central role in the microalgal primary metabolism and originates fundamental precursors feeding the synthesis of carbohydrates, proteins or fatty acids (Ho et al., 2014; Zhao and Su, 2014). In most photosynthetic organisms, starch and other polysaccharides are the primary form of temporary accumulated macromolecules with high energetic content (Stitt and Zeeman, 2012; Vitová et al., 2015). However, some species of microalgae are highly efficient in accumulating triacylglycerols (TAGs) in lipid bodies in the cytosol by a metabolic pathway that is highly coordinated across the chloroplast, the endoplasmic reticulum and the cytosol itself (Radakovits et al., 2010; Bogen et al., 2013; Poliner et al., 2015). Some of these microalgae species can accumulate lipids up to 60% of their dry weight (Hu et al., 2008), and for this reason, they have attracted attention as a possible feedstock for the production of biofuels. In this context, particular interest is raised by species of the *Nannochloropsis* genus, unicellular photosynthetic microalgae belonging to the Eustigmatophyceae and distributed worldwide in marine, fresh, and brackish waters, capable of massive lipid accumulation (Meng et al., 2015; Slocombe

et al., 2015), especially under nutrient deprivation (Boussiba et al., 1987; Rodolfi et al., 2009).

Because of these properties, *Nannochloropsis* is an interesting model for understanding how different organisms regulate metabolic fluxes toward lipid or carbohydrate synthesis. In *Nannochloropsis*, the ability to synthesize lipids is supported by a genomic enrichment in biosynthesis genes and glycoside hydrolases that should play a role in shifting carbon fluxes toward TAG metabolism. An example of this expansion is the *Diacylglycerol acyltransferase-2* (*DGAT-2*) genes, which in *Nannochloropsis* species investigated showed 11 copies. As a comparison, diatoms such as *Thalassiosira pseudonana* or *Phaeodactylum tricornutum* have four *DGAT-2* copies, while the green alga *Chlamydomonas reinhardtii* has five *DGAT-2* genes, despite all having much larger genomes than *Nannochloropsis* (Wang et al., 2014).

Lipid accumulation in several algal species is triggered by nitrogen (N) depletion, and these conditions have been heavily investigated to understand lipid metabolism regulation (Miller et al., 2010; Simionato et al., 2013; Li et al., 2014; Lu et al., 2014; Martin et al., 2014; Abida et al., 2015; Jia et al., 2015). Nitrogen deprivation also leads to accumulation of storage sugars like starch or chrysolaminarin, depending on the organism (Jia et al., 2015), and the impairment of the storage sugar metabolism was observed to further increase TAGs (Blaby et al., 2013). However, N depletion also causes a major impairment of the basic metabolism, shutting down nucleic acid and protein biosynthesis and limiting cell division and growth (Simionato et al., 2013). Upon nitrogen shortage, the fatty acids required for TAG accumulation in *Nannochloropsis gaditana* are mostly produced de novo with, nevertheless, a significant contribution of galactolipids recycled from degraded thylakoid membranes (Simionato et al., 2013). Investigating other stimuli capable of inducing TAG biosynthesis could thus be highly valuable to disentangle the nitrogen depletion response and identify metabolic switches that induce lipid accumulation without depressing biomass growth.

It has been shown that light can induce lipid accumulation in *Nannochloropsis salina* (Sforza et al., 2012), and since photosynthesis is the primary source of all reduced carbon, it is understandable that light is a master regulator of metabolism. Broadly speaking, lipid biosynthesis and management depend on the production and recycling of photosynthates. Investigating the metabolic remodeling following light treatment and understanding the crosstalk between the metabolic pathways in response to light changes can thus clarify how carbon partitioning is modulated.

To this end, we investigated the light response of *N. gaditana* cultures, combining a genome-wide transcriptional analysis with lipidomic, metabolomic, and functional approaches. The results showed that the lipid accumulation induced by strong illumination is consistent with the coordinated activation of the putative fatty acid biosynthesis in the cytoplasm/endoplasmic reticulum (ER) and the parallel inhibition of the chloroplast

fatty acid biosynthesis. This process is accompanied by increased carbon fluxes out of the chloroplast, shifting the balance toward the ER and TAGs accumulation.

RESULTS AND DISCUSSION

N. gaditana in Limiting and Excess Light Conditions

Cells of *N. gaditana* strain CCAP 849/5 were cultivated in small-scale photobioreactors at three different light intensities: low (LL; $10 \mu\text{mol photons m}^{-2} \text{s}^{-1}$), medium (ML; $100 \mu\text{mol photons m}^{-2} \text{s}^{-1}$), and high (HL; $1000 \mu\text{mol photons m}^{-2} \text{s}^{-1}$) light. Cell duplication was continuously monitored throughout the 5 d of growth by measuring OD_{720} (Fig. 1A). ML cultures showed the fastest growth, as expected (Sforza et al., 2012), while LL cells were light limited. Cells under HL conditions also showed slower growth compared to ML, suggesting a photoinhibitory effect (Fig. 1A; Simionato et al., 2011; Sforza et al., 2012), as supported by the progressive reduction in PSII maximum quantum efficiency (F_v/F_m) observed when increasing the light regime (Fig. 1B). Growth differences in response to light availability were also confirmed by measuring cell concentration (Fig. 1C) and dry weight (Supplemental Fig. S2) after 5 d. Nile Red staining showed that after 5 d of light treatment, neutral lipid accumulation was induced by 4-fold in the ML and HL cells compared to LL (Fig. 1D). This result is consistent with the literature showing enhanced TAG accumulation for *Nannochloropsis* in response to increased light intensity if CO_2 is not limiting (Pal et al., 2011; Sforza et al., 2012; Teo et al., 2014). To better understand how light intensity affects the *N. gaditana* metabolism and induces heightened lipid accumulation, the same cells grown for 5 d under different light intensities were subjected to transcriptomic, metabolomic, lipidomic, and functional analyses.

Genome-Wide Changes in mRNA Abundance in Response to Light

An mRNA-seq experiment was performed with three biological replicates to measure the response of *N. gaditana* to the three different light intensities. Out of 10,919 total predicted nuclear genes (Corteggiani Carpinelli et al., 2014), transcripts of 10,456 genes were detected under the three conditions. For the functional classification of light response, we chose those genes showing statistically significant differential expression (see "Materials and Methods" for details). A total of 2,354 genes were differentially expressed between LL- and ML-grown cells and 4,673 between LL- and HL-grown cells. A lower number of genes (639) were differentially expressed between ML- and HL-grown cells, suggesting that overall the ML transcriptome was closer to HL than to LL conditions (Fig. 2; Supplemental Fig. S3). Only 69 genes were down-regulated in both conditions, and 18 genes were up-regulated in both conditions, representing the core of genes progressively activated and

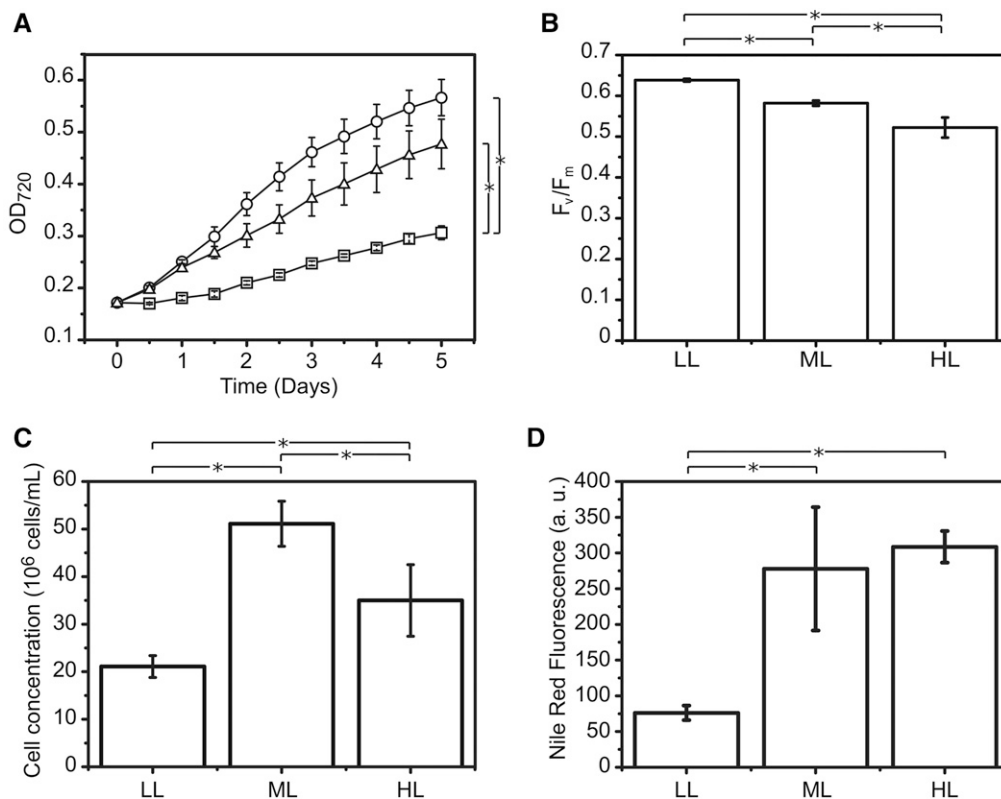


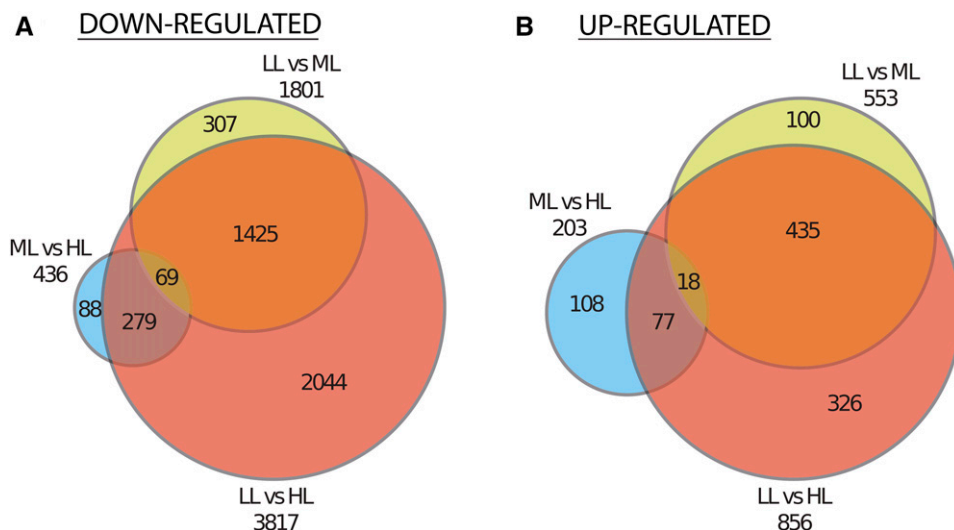
Figure 1. Light effect on the growth and lipid accumulation of *N. gaditana* cells. A, Growth curves of wild-type cells during the 5 d of differential light treatment. Squares, low light; circles, medium light; triangles, high light. At day 5, cells were harvested to measure the following parameters: PSII quantum yield (F_v/F_m ; B), cell concentration (C), and neutral lipid accumulation determined by fluorescence spectra analysis of Nile Red-stained cells (D). a.u., Arbitrary units and the values are normalized to the same cell number (see “Materials and Methods” for details). A saturating light pulses of 0.6 s at 6,000 μmol of photons $\text{m}^{-2} \text{s}^{-1}$ was used to measure F_m . Data are expressed as average of three biological replicates \pm SD. Asterisks indicate statistical significant differences by one-way ANOVA, P value < 0.05.

gradually turned off by increasing light availability, respectively (Fig. 2; Supplemental Data Set S1).

The differentially expressed genes were clustered into six groups on the basis of their expression levels (Fig. 3A; see Supplemental Note S1 for details).

Different clusters were subjected to Gene Ontology enrichment analysis using the blast2go software (Supplemental Note S1), integrated with a manual annotation, distributing the genes of each cluster into 14 major functional groups (Fig. 3B; Supplemental Fig. S4).

Figure 2. Venn diagrams of differentially expressed genes identified in the three light conditions. A, Genes down-regulated in LL versus ML are compared with genes down-regulated in ML versus HL and LL versus HL. Out of the 639 genes differentially regulated between ML and HL, 146 (23%) were specific to this comparison. (B) Genes up-regulated in LL versus ML are compared with genes up-regulated in ML versus HL and LL versus HL. Out of the 2,354 LL versus ML regulated genes, only 398 (16%) were specific to this comparison.



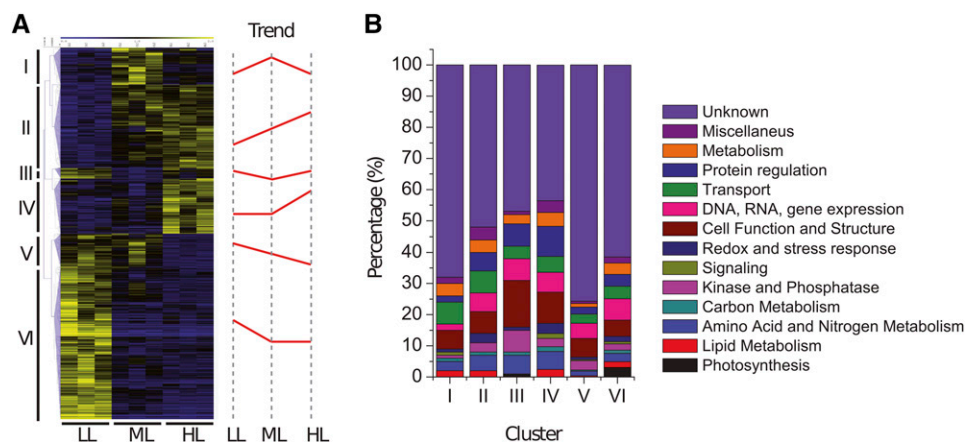


Figure 3. Hierarchical clustering of light regulated genes. A, A transcriptional profile dendrogram was created using TMeV 4.3 software. Six groups have been highlighted on the left side of the picture. The red lines on the right side represent schematically the overall trend of light response of the genes belonging to the corresponding cluster. B, Manual annotation and category distribution among clusters. Manual annotation was done on the base of gene description and Gene Ontology (biological process). The genes in A were grouped according to their function in 14 categories: photosynthesis, lipid metabolism, amino acid and nitrogen metabolism, carbon metabolism, kinase and phosphatase, signaling, redox and stress response, cell function and structure, DNA/RNA/gene expression, transport, protein regulation, metabolism, miscellaneous, and unknown. Protein domains that could not be classified in any specific category were grouped into the “miscellaneous” category. The “unknown” category refers to protein sequences for which no consensus was reachable through annotation. Percentage of each functional category is represented in the total numbers of differentially expressed transcripts from each individual set of data.

In all cases, genes with unknown function were the most represented class, constituting between 44 and 73% of the genes in each cluster, showing that the function of a large fraction of *N. gaditana* genes cannot be easily deduced from annotation. In some cases, however, we were able to identify specific profiles, such as for those genes involved in photosynthesis which were enriched in cluster VI and therefore up-regulated in LL compared to ML and HL. Genes involved in lipid metabolism were instead more abundant in clusters I, II, and IV, meaning they are up-regulated in ML and HL compared to LL, in accordance with the higher lipid accumulation reported in Figure 1D. Genes involved in redox and stress response were more abundant in clusters II and IV, suggesting the activation of an oxidative stress response at the transcriptional level in *N. gaditana* exposed to excess light (Figs. 1B and 3; Supplemental Fig. S4).

Starting from the results of cluster analysis, a selection of gene families and metabolic pathways was analyzed in greater detail, complementing the gene expression data with metabolic and functional analyses.

Modulation of Photosynthetic Apparatus in Response to Different Light Intensities

Photosynthetic organisms react to different light regimes by modulating their photosynthetic apparatus both in protein and pigment content (Maxwell et al., 1994; Bailey et al., 2001; Dietz, 2015). In agreement with the general reduction of gene expression in the biosynthetic pathway of chlorophyll and carotenoids (Supplemental Note S2), their total amount per cell

decreased in proportion to increasing light intensity (Table I). We consistently observed a strong and generalized decrease in the expression of genes of the Light-Harvesting Complex (LHC) superfamily, which encodes the proteins constituting the antenna system of the photosynthetic apparatus in eukaryotes. The only exception to this general behavior was the gene *Naga_101036g3*, which was significantly up-regulated in ML and HL with respect to LL conditions (Fig. 4A; Supplemental Data Set S2A). The biological function of LHC proteins can be measured by determining the functional antenna size of PSII (ASII), based on chlorophyll fluorescence (see “Materials and Methods” for details). ASII increased in cells grown in LL compared to ML and HL conditions (Fig. 4B), confirming that LHC expression is enhanced in LL-treated cells of *N. gaditana* to maximize light harvesting capacity.

LHC proteins from *Nannochloropsis* can be classified into three subgroups (Vieler et al., 2012), with LHCF and LHCR composing the main antenna proteins, as in

Table 1. Changes in chlorophyll-a and total carotenoid content in *N. gaditana* cells at different light regimes

Data are all expressed as average of three biological replicates \pm sd. Each sample was significantly different from the other (one-way ANOVA plus Tukey's *t* test, *P* value < 0.05). Chl, Chlorophyll; Car, carotenoid.

Sample	Chl (pg)/Cell	Car (pg)/Cell	Chl/Car
LL	0.133 \pm 0.006	0.0389 \pm 0.0012	3.42 \pm 0.05
ML	0.063 \pm 0.005	0.0239 \pm 0.0017	2.65 \pm 0.04
HL	0.038 \pm 0.006	0.0184 \pm 0.0018	2.04 \pm 0.14

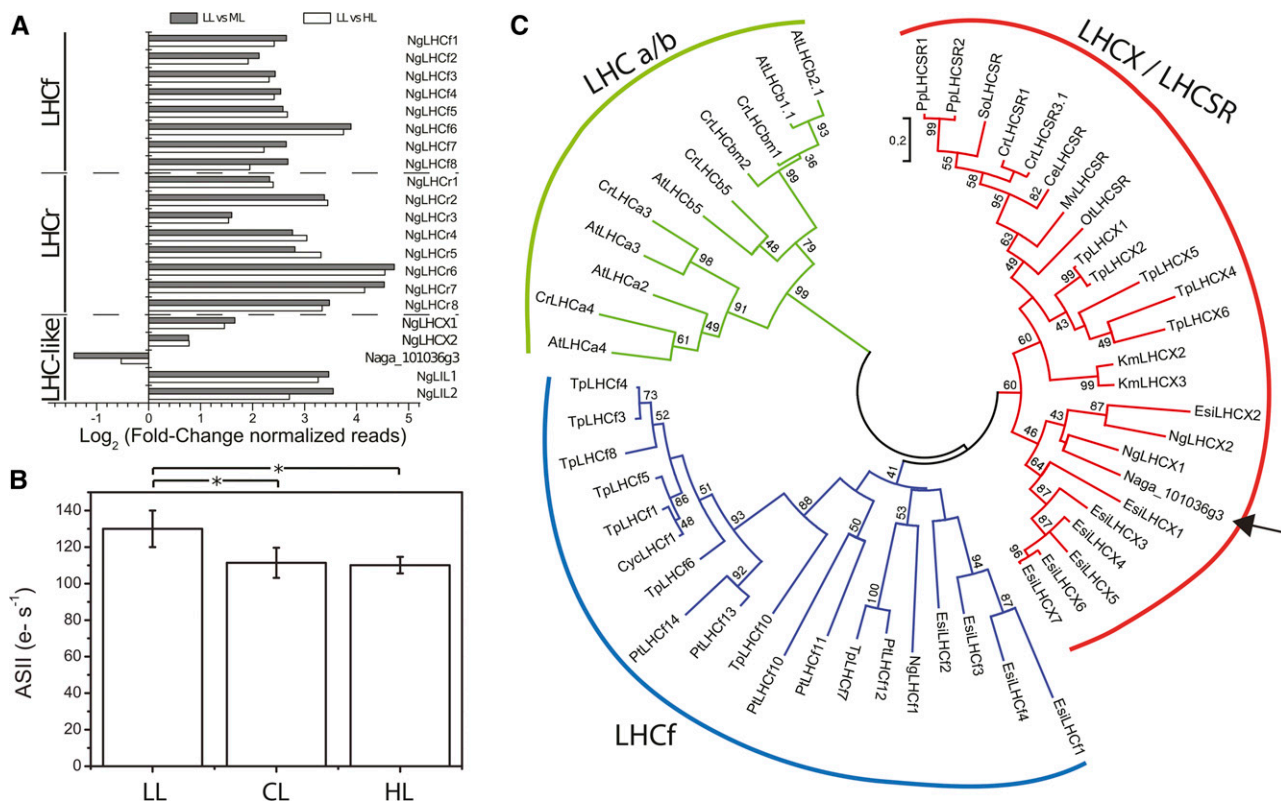


Figure 4. Regulation of LHC complexes. A, Gene expression regulation of *LHC* superfamily members. Gray and white bars represent the fold change of normalized reads of LL versus ML and LL versus HL, respectively. For each sample, the average of normalized reads of three repetitions was used to calculate the fold change, which is expressed in log₂ scale. All genes except Naga_100056g42 (*NgLHCX2*) are significantly regulated in response to light in the reported comparisons. B, Functional antenna size of PSII measured by fluorescence induction kinetics monitored upon excitation with 320 μmol photons m⁻² s⁻¹ of actinic light at 630 nm. Data are all expressed as average of three biological replicates ± SD. Asterisks indicate statistical significant differences by one-way ANOVA, *P* value < 0.05. C, Phylogenetic tree of LHC superfamily. Naga_101036g3 gene model was translated to the corresponding protein sequence for a tBLASTn analysis in the NCBI nucleotide collection. To attribute Naga_101036g3 to a specific subgroup of LHC, its primary sequence was compared to a larger number of LHC protein sequences, notably, 11 LHC proteins of chlorophyll a/b-containing organisms, 19 LHCf proteins, and 23 LHCX/LHCSR photoprotective proteins from different algae. A multiple alignment of these 52 full-length protein sequences was performed using MUSCLE, and the aligned protein sequences were used to construct an unrooted maximum likelihood phylogenetic tree using MEGA6.0. Sequence alignment and details are given in Supplemental Figure S1.

diatoms and brown algae, and found associated predominantly but not exclusively with the PSI and PSII complexes (De Martino et al., 2000; Beer et al., 2006; Lepetit et al., 2007; Ikeda et al., 2013). A third group, LHCSR or LHCX, instead consists of antennas involved in photoprotection and stress response in several algae species and mosses (Richard et al., 2000; Peers et al., 2009; Alboresi et al., 2010; Zhu and Green, 2010). To infer Naga_101036g3 putative function from its primary sequence, protein BLAST searches retrieved sequences annotated as LHCSR in the top hits (e-value < 10⁻³⁴). This assignment is confirmed by the phylogenetic tree, showing that Naga_101036g3 appeared to be part of the LHCX/LHCSR subgroup together with two other putative LHCX proteins of *N. gaditana* (i.e. Naga_100173g12 and Naga_100056g42, respectively, NgLHCX1 and NgLHCX2; Fig. 4C).

The similarity of Naga_101036g3 to the LHCX proteins and its peculiar up-regulation in stronger light (Fig. 4A) suggested that this gene may have a specific role in response to strong light intensities. Interestingly, however, the two other LHCX genes identified in the *N. gaditana* genome exhibited similar expression profiles to other antennas (Fig. 4A; Supplemental Data Set S2A).

Regulation of Genes Involved in Lipid Metabolism

Most of the genes putatively involved in lipid biosynthetic pathways have been previously annotated for *Nannochloropsis* (Vieler et al., 2012; Corteggiani Carpinelli et al., 2014; Li et al., 2014), showing that lipid biosynthesis follows a complex pathway extended across several compartments. In photosynthetic eukaryotes, fatty acids (FAs) are synthesized in the chloroplast

stroma; thylakoid lipids (monogalactosyldiacylglycerol [MGDG], digalactosyldiacylglycerol [DGDG], sulfoquinovosyldiacylglycerol [SQDG], and phosphatidylglycerol [PG]) are synthesized in chloroplast envelope membranes; major phospho-glycerolipids (e.g. phosphatidylcholine [PC] and phosphatidylethanolamine [PE]), betaine lipids (diacylglyceryltrimethylhomo-Ser [DGTS]) and TAGs are instead synthesized in the ER (Petroustos et al., 2014). Based on genomic evidence, the metabolic pathways for the production of glycerolipids are expected to follow this general scheme in *Nannochloropsis*. One remarkable feature of FA synthesis, however, differentiates *Nannochloropsis* from other photosynthetic eukaryotes, since genes coding for cytosolic proteins that could act as a fatty acid synthase of type 1 (*FAS1*) or a polyketide synthase (*PKS*) have also been identified (Vieler et al., 2012). Based on a phylogenetic analysis using three *FAS1/PKS*-like gene sequences from *Nannochloropsis oceanica*, it was recently proposed that these proteins were more similar to fungal polyketide synthases than to *FAS1* (Poliner et al., 2015).

In cells exposed to different illumination intensities, we observed the statistically significant down-regulation of several lipid biosynthesis genes coding for proteins localized in the chloroplast. In fact, genes coding for components of the chloroplast *FAS2* were less expressed in ML and HL (*BXP1*, Naga_100594g3; *MCT*, Naga_100046g34; *KAR1*, Naga_100037g12; *HAD1*, Naga_100113g7, *ENR1*, Naga_101525g2; Supplemental Data Set S3B). By the same token, the gene coding for cytosolic acetyl-CoA carboxylase (*ACC1*, Naga_100605g1) was down-regulated under the ML and HL conditions. In contrast with the down-regulation of genes encoding plastid *FAS2* components, we detected the up-regulation in HL of two β -ketoacyl synthases (Naga_102909g1 and Naga_101811g1) and five polyketide synthases (Naga_102303g1, Naga_102722g1, Naga_101380g1, Naga_103117g1, and Naga_100022g68), all predicted to be localized in the cytosol (Supplemental Data Set S3B), suggesting a remodulation of lipid biosynthesis with cytosolic fatty acid synthesis, increasing its relevance at the expense of the chloroplast.

Second, we detected a general up-regulation of genes involved in thylakoid lipid assembly in the chloroplast, i.e. lyso-phosphatidic acid and phosphatidic acid (*GPAT*, also known as *ATS1*, Naga_100562g3), diacylglycerol (*PAP*, Naga_100075g9), PG (*CDS1*, Naga_100056g35; *PGPS*, Naga_100114g5), SQDG (*SQD1*, Naga_100038g9), and galactolipids (*MGD1*, Naga_100092g7) (Supplemental Data Set S3B). This feature is different from what was reported recently in *N. oceanica* along a circadian rhythm (Poliner et al., 2015), in which the expression of the plastid glycerolipid genes (genes involved in the synthesis of diacylglycerol (DAG), MGDG, DGDG, and SQDG) displayed high coordination with FA synthesis genes at the transcriptional level so that their expression preceded the observed lipid accumulation during the daylight period. Although we cannot exclude the existence of a previous unrecorded phase of up-regulation of *FAS2* genes, the HL regime seems to disrupt this coordination.

Third, in membrane glycerolipid biosynthesis in the ER, two putative genes coding for enzymes producing phospho-choline (Naga-100331g3 and Naga_100090g21), the polar head used for PC synthesis, were less expressed in ML and HL. By contrast, two genes putatively encoding betaine lipid synthesizing enzymes (*BTA1*, Naga_100016g36 and Naga_100004g72) were up-regulated.

Instead, in storage glycerolipid biosynthesis in the ER, we detected a significant up-regulation of the expression of several diacylglycerol-acyltransferase (*DGAT*) genes in ML and HL compared to LL, suggesting increased synthesis of these lipids. More precisely, *DGAT1* (Naga_101968g1) is the most up-regulated *DGAT* gene in response to increasing light ($FC_{LL \text{ vs } ML} = -1.12$; Supplemental Data Set S3B).

Out of the 11 *DGAT2* genes present in the genome, three were more highly expressed in ML and HL than LL (*DGAT2a*, Naga_100343g3; *DGAT2b*, Naga_100010g31; *DGAT2f*, Naga_100006g86), while two are more specifically induced in HL compared to LL (*DGAT2h*, Naga_100010g4; *DGAT2k*, Naga_100004g173). A phospholipid:diacylglycerol acyltransferase that acts by transferring an acyl group from a phospholipid to DAG, thus producing TAG, is also up-regulated in ML and HL (*PDAT*, Naga_100065g17; Supplemental Data Set S3B). Taken together, these data suggest a general increase in ER-localized TAG biosynthesis.

The subgroup of desaturases showed a peculiar behavior, with expression levels peaking in ML conditions and lower expression in both LL and HL (Supplemental Data Set S3B and see Supplemental Note S3 for details).

Several genes classified as involved in lipid catabolism are expressed more in HL than in LL but also in ML compared to LL (Supplemental Data Set S3B), with the strongest up-regulation observed for a lipase ($FC_{LL \text{ vs } ML} = -2.37$, $FC_{LL \text{ vs } HL} = -3.07$; Naga_100040g9). Out of 76 putative genes involved in lipid catabolism, only three are expressed at higher levels in LL than ML or HL, namely, one dehydratase (Naga_100034g21), one AMP-dependent synthetase and ligase (Naga_100012g66), and one phospholipase A2 (Naga_100247g4). As recently reported for the oleaginous diatom *Fistulifera solaris* under N shortage (Tanaka et al., 2015), some genes involved in fatty acid beta-oxidation in the mitochondria have a higher expression level in conditions that trigger TAG accumulation, i.e. in ML and HL (*KAS4*, Naga_100004g8, *HAD2*, Naga_100486g4, *ENR2*, Naga_100016g22).

In summary, gene expression analysis suggests that lipid biosynthesis is down-regulated in the chloroplast in response to increased light, while genes involved in cytoplasmic fatty acid synthesis as well as the insertion of fatty acids into TAG are induced.

Regulation of Lipid Accumulation

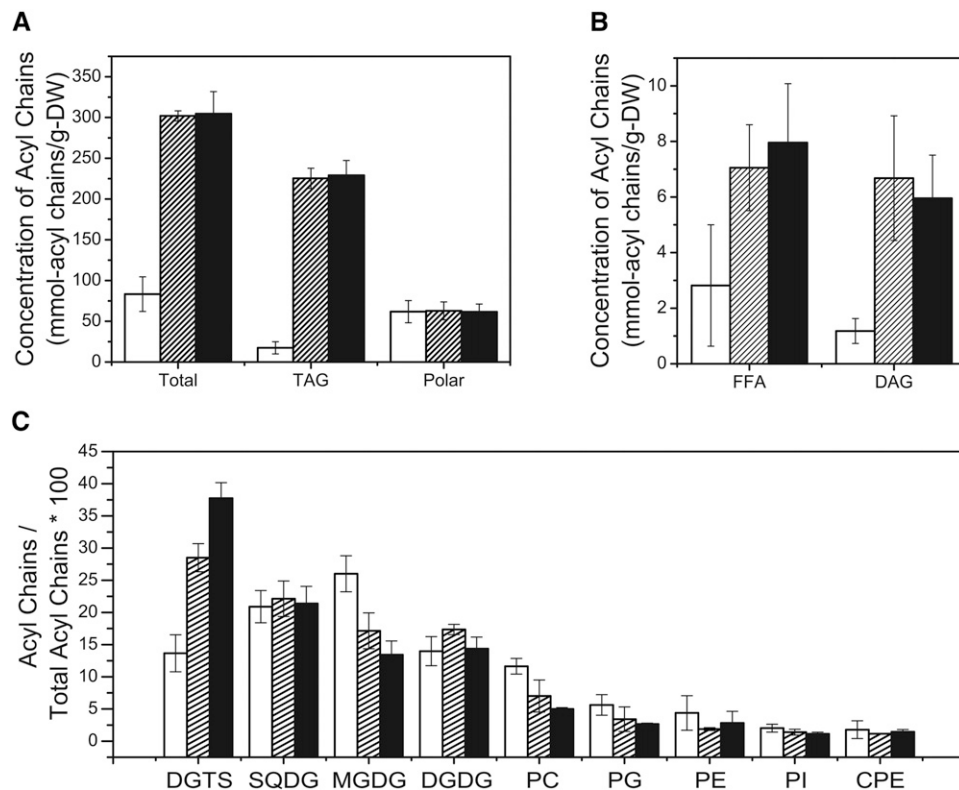
A lipidomic analysis was performed to characterize how lipid accumulation correlated with gene

regulation (Fig. 5). It is worth noting here that the same independent batches of cells were used for the mRNA-seq, lipidomic, and metabolomic analyses (see “Materials and Methods” for details) to make all the results directly comparable. The total amount of acyl lipids was higher in ML and HL than in LL (Fig. 5A), consistent with Nile Red quantification (Fig. 1D). The step between ML and HL did not trigger any significant change in overall lipid content (Fig. 5A), suggesting that the light-dependent induction of TAG accumulation is already activated in ML cultures. Interestingly, while the content of polar lipids was not significantly affected, the acyl lipid increase was completely due to the larger TAG accumulation. This increase in TAG suggests that fatty acid production is activated by increased light intensity, in contrast with the observed down-regulation of genes encoding plastid FAS2. This result suggests that the increased production of fatty acids relies on the activity of the cytosolic FAS1 system, most notably on the FAS1/PKS-like protein (Naga_100022g68), whose expression increases at higher light intensities (Supplemental Data Set S3B).

DAGs, the likely precursors of TAG biosynthesis, are accumulated 50 times less than TAG, but the two lipid classes show a similar response to light intensity with the induction of DAG accumulation in ML and HL (Fig. 5B). This result suggests that precursors of TAG biosynthesis are accumulated together with the final product. Based on the transcriptome analyses, both the de novo synthesis of TAG (via DGAT enzymes) and phospholipid recycling (via PDAT) are likely to drive TAG accumulation.

We also analyzed the different classes of membrane lipids, observing some significant changes among the three light intensities (Fig. 5C). The most notable one is a gradual and strong increase of DGTS from LL to ML and HL. In contrast, PC decreased in HL, possibly counterbalancing the variations in DGTS content (Fig. 5C). Concerning plastid lipids, whereas MGDG decreased, DGDG and SQDG remained stable, and PG decreased moderately. Even if the precise DGTS role in HL is unclear, this result is extremely interesting because it means that specific polar lipids are differentially accumulated in response to light, even though the total amount of the polar fraction is not altered. It is also worth emphasizing that there is a relationship between the regulation of polar lipid accumulation and the compartmentalization of the corresponding biosynthetic pathway. In fact, DGTS is likely synthesized in the endoplasmic reticulum from DAGs by a BTA enzyme that is up-regulated at the transcriptional level (Supplemental Data Set S3B). As synthesis of PC relies on phospho-choline, its decrease might also be correlated with a decline in the genes coding for enzymes that produce phospho-choline. The synthesis of chloroplast lipids might result from the combination of opposite trends, i.e. a decline in fatty acids synthesized by FAS2 components encoded by down-regulated genes (*KAR1*, *HAD1*, and *ENR1*; Supplemental Data Set S3B) and a stable or increased expression of genes involved in thylakoid lipid assembly (*GPAT/ATS1*, *PAP*, *CDS1*, *PGPS*, *SQD1*, *MGD1*, and *DGD1*; Supplemental Data Set S3B), resulting in an overall stability of SQDG

Figure 5. Glycerolipid remodeling in response to light intensity. Lipid profiling was performed on *Nannochloropsis* cells grown for 5 d under three different light conditions. Concentration of total lipids, triacylglycerols, and polar lipids (A) and concentration of free fatty acids and diacylglycerols (B) are reported on two independent panels with different scales. Their concentration is reported as moles of acyl chains on dry weight (DW). C, Relative accumulation of each class of polar lipid on the total amount of polar lipids. The different classes of polar lipids are arranged from the most to the less abundant in ML. White bars, LL; striped bars, ML; black bars, HL. Data are all expressed as average of three biological replicates. Error bars correspond to sd of three biological replicates. Total, total lipids; Polar, polar lipids; FFA, free fatty acids; PI, phosphatidylinositol; CPE, carboxymethyl phosphatidylethanolamine.



and DGDG, a slight decrease in PG and a decline in MGDG.

The specific increase of the betaine lipid triggered by light intensity brings up the question on how DGTS accumulation in HL could be supported if plastid fatty acid biosynthesis is inhibited. Again, a possible explanation for this finding lies in the identification of cytosolic *FAS1/PKS*-like genes (Naga_100022g68, Naga_100001g49, and Naga_100028g49; Supplemental Data Set S3B), which are also induced in HL. This result suggests that upon light stimulus, DGTS accumulation is also increased by the activation of cytosolic fatty acid biosynthesis, compensating for the decrease in plastid pathway activity. This possibility of supporting lipid biosynthesis in two different compartments provides a high flexibility to *N. gaditana* that would allow it to finely regulate fatty acid biosynthesis in response to environmental stimuli, as observed here. This organism also represents the first described photoautotroph capable of this separation (Ramakrishnan et al., 2013; Petroustos et al., 2014).

When we analyzed the acyl profiles of each lipid class, some variations in 16:0, 16:1, and 20:5 could be observed in most membrane lipids, with the exception of SQDG. Most lipids with 16:1 acyl-groups are generated through the neosynthesis of fatty acids in the plastid by the stearyl-ACP desaturase (actually acting as a palmitoyl-ACP desaturase). An exception is 16:1 in PG, which is synthesized by an alternative pathway as a transdouble bond rather than a cis-double bond (= 16:1t).

Concerning light-dependent regulations, HL induces a relative decrease in 16:1 and an increase in 20:5 in plastid galactolipids (MGDG and DGDG), while LL triggers an opposite effect. It is interesting to note that, although in HL there is an excess of electrons and oxidative conditions (Fig. 1, A and B), MGDG and DGDG, the lipids most exposed to this stress in the thylakoids, contain more unsaturated species. Either these species play a role in response to oxidation or a mechanism protecting these polyunsaturated lipids is established.

It is worth mentioning that LL samples are characterized by an increase of 16:1 membrane lipids, probably because the demand for TAG biosynthesis is not strong enough and the newly synthesized 16:1 lipids are dedicated to feeding MGDG, DGDG, and PC (Fig. 6).

We also observed significant changes in PG under HL, with an increase in 16:1 in favor of 16:0. PG is found in different cellular compartments and in particular in the thylakoids, where it contains 16:1t, and in the ER, where PG is devoid of 16:1t. In the thylakoids, the 16:1t acyl group of PG was shown to be critical for association with photosystems, particularly the D1 core of PSII (Endo et al., 2015). The observed increase of PG with higher proportions of 16:1t when light intensity increases is thus possibly playing a role in PSII protection. This result is consistent with the evidence in Figure 1B that HL cells suffer from significant PSII photo-inhibition, increasing their need for PSII repair.

Although they likely follow independent mechanisms, this modification in PG, together with the DGTS variation mentioned earlier, can be considered as hallmarks of the response to the light increase.

The acyl distribution of TAGs followed the same trend observed in DAGs, with a limited amount of 20:5, suggesting that the fatty acids are not recycled from polar lipids but originate entirely from de novo synthesis. This finding is significantly different from the observations in nitrogen-depleted cells, where even if neosynthesis played a major role in sustaining TAG production, there was clear evidence of fatty acid recycling from the polar lipids coinciding with the degradation of thylakoids (Simionato et al., 2013).

Regulation of Triose, Pentose, and Hexose Content

We analyzed the regulation of the genes belonging to those pathways directly involved in primary carbon metabolism, which will necessarily feed all other metabolic pathways (Supplemental Data Set S3A). Glycolysis and the Calvin-Benson cycle are involved in the metabolism of hexose molecules, essential building blocks for all biomolecules. Deciphering the regulation of metabolic response in microalgae is extremely complex because of the overlap among pathways and because of their sophisticated compartmentalization (Johnson and Alric, 2013; Li et al., 2014). The collection of genome-wide data from different environmental conditions is essential to entangle this complex metabolism and its various crosstalk.

Among the significant regulations identified in the conditions analyzed here, glucokinases (*GK*; Naga_100170g2 and Naga_100119g19) are up-regulated in ML and HL, while the cytosolic phosphoglucose isomerase is strongly up-regulated in LL (*GPI*; Naga_100305g6). Phosphofructose kinase (*PFK*) and aldolases (*ALDO*) did not show any transcriptional regulation, but a strong response to light was found for the group of eight Fru bisphosphatases. Two of them (Naga_100005g122 and Naga_100159g16) were up-regulated in HL, while three were down-regulated in HL (Naga_101891g1, Naga_102887g1, and Naga_100005g28). Interestingly, in silico analysis of their coding sequences suggested a cytosolic localization for up-regulated sequences and a plastid localization for down-regulated sequences. High expression of Fru bisphosphatase in the cytosol could serve for the synthesis of storage carbohydrates (likely 1,3- β -glucans, known as chrysolaminarin or laminarin in *Nannochloropsis*; Jia et al., 2015), while its low expression in the plastid could avoid the removal of Fru 1,6-bisphosphate from the glycolytic pathway.

Through glycolysis, hexose phosphates are broken down into three-carbon intermediates by the action of aldolases, producing DHAP and GAP, two compounds that are interconverted by the action of triose phosphate isomerases (TPI). DHAP and GAP are essential molecules in the metabolism, being intermediates in various metabolic pathways located in different compartments

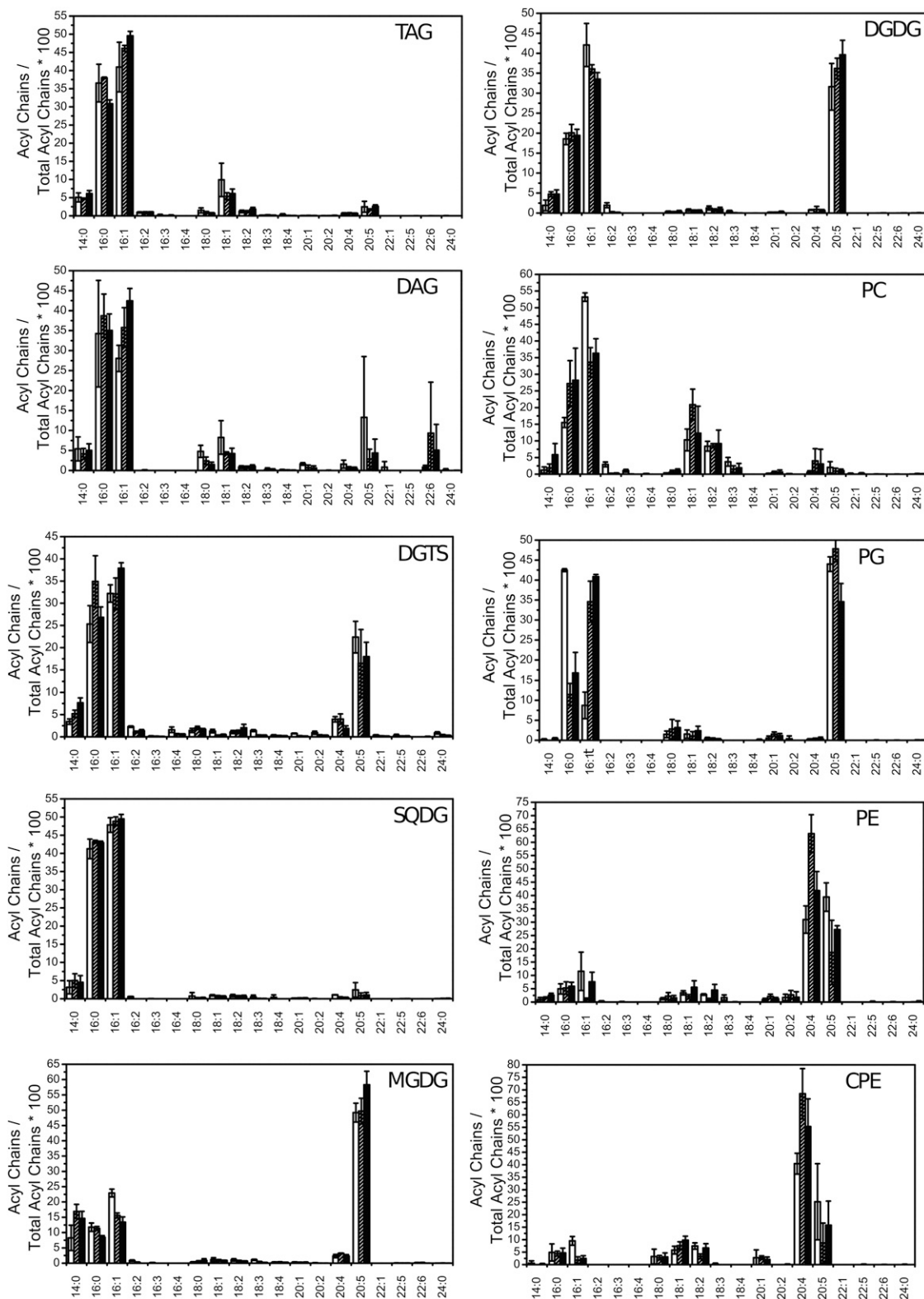


Figure 6. Estimated acyl chain composition as a function of lipid class. Data are all expressed as average of three biological replicates. Error bars correspond to *sd* of three biological replicates. Data are arranged from the most to the less abundant lipid class (from the top to the bottom of the left and right columns), according to the quantification reported in Figure 5. White bars, LL; striped bars, ML; black bars, HL. CPE, carboxymethyl phosphatidylethanolamine.

of the cell, including glycolysis in the chloroplast, mitochondrion, or cytosol, the Calvin-Benson cycle in the chloroplast, or the pentose phosphate pathway (Chen and Thelen, 2010; Zaffagnini et al., 2014). DHAP is also a main precursor for IPP biosynthesis via the non-mevalonate pathway in the chloroplast (Supplemental Note S1), namely, the precursor for isoprenoids, which are severely down-regulated under HL. Interestingly, one of the major conclusions of a recently reported study on circadian transcriptional regulation in *N. oceanica* was that a coordination between the glycolysis and fatty acid synthesis occurred for lipid production (Poliner et al., 2015). Out of three triose phosphate isomerase sequences, one is down-regulated in ML (*TPI*, Naga_100011g1), while the two others (Naga_103287g1 and Naga_100001g84) are up-regulated in ML and HL compared to LL. The down-regulated enzyme, involved in the Calvin-Benson cycle, is localized in the chloroplast, while the up-regulated ones are cytosolic and participate in glycolysis. An altered coupling of photosynthesis and glycolysis therefore seems

to be supported by these data, with a cytosolic energetic metabolism relying on hexose phosphate consumption.

To complement the expression data, the light response of primary carbon metabolites, trioses, pentoses, and hexoses, was quantified (LC-HRMS; see “Materials and Methods” for details; Fig. 7; Supplemental Data Set S4). For most sugars, there is a generalized increase in accumulation with light intensity, and 13 out of 23 measured carbohydrates were significantly more abundant under ML compared to LL (Fig. 7; Supplemental Data Set S4). In particular, maltotriose responds progressively to light (LL < ML < HL; Fig. 7A). Similarly, sorbitol/mannitol and Fru-dianhydride are accumulated in response to increased light. The sugar accumulation signature in HL could negatively regulate photosynthesis and Calvin-Benson cycle gene expression (Couée et al., 2006; Supplemental Data Set S3A), as reported in several plant and cyanobacteria species when exposed to high light conditions (Pego et al., 2000; Rolland et al., 2006). In other photosynthetic organisms, sugar accumulation has also been correlated with the down-regulation of

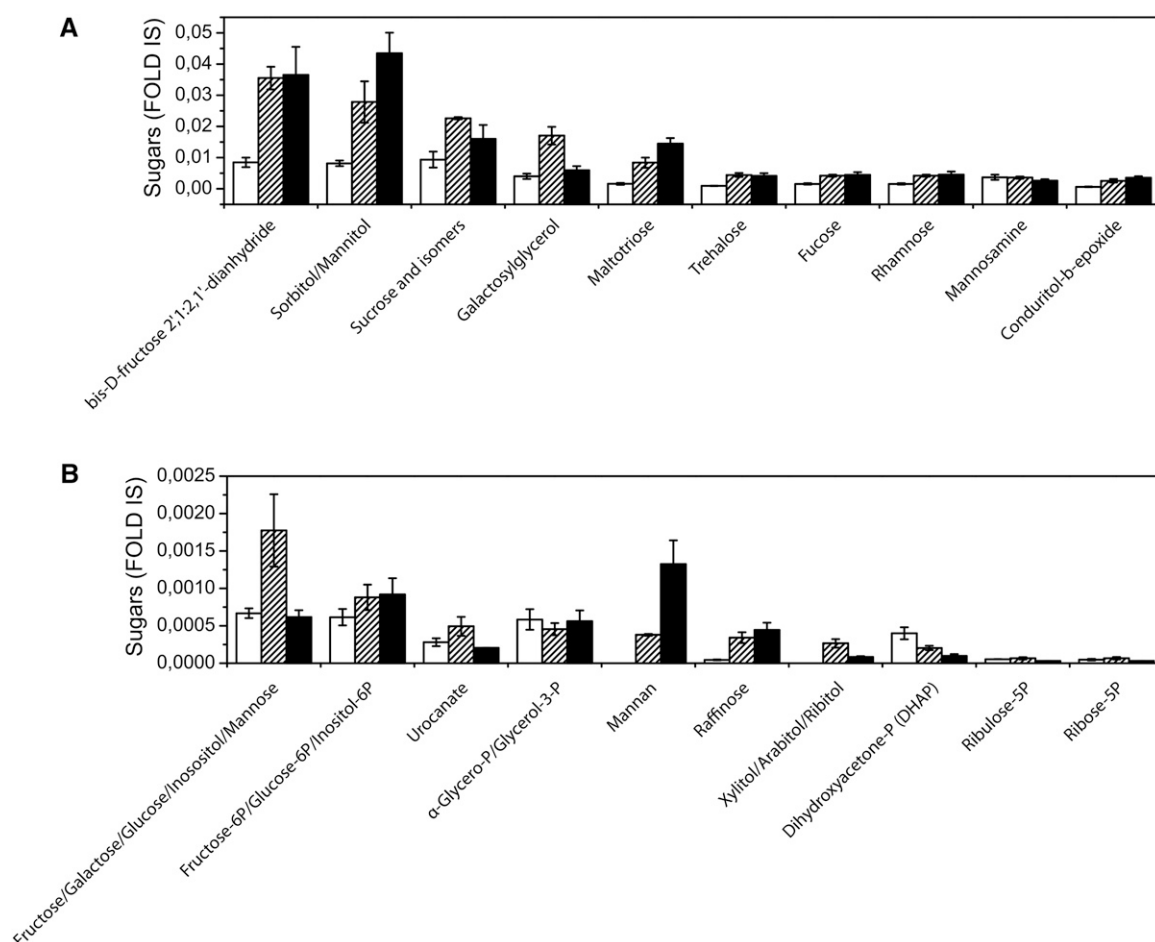


Figure 7. LC-ESI(+)-MS analyses of sugars in *N. gaditana* cells grown in different light conditions. Data are expressed as relative content with respect to the level of the internal standard (formononetin). White bars, LL; striped bars, ML; black bars, HL. Data are all expressed as average of three biological replicates. Error bars correspond to SD of three biological replicates. For more details, see “Materials and Methods.”

peroxisomal lipid β -oxidation (Contento et al., 2004), carotenoid biosynthesis (Ryu et al., 2004), and reactive oxygen species scavenging processes (Stoop et al., 1996; Elbein et al., 2003; Lunn et al., 2014), all phenomena also observed in this work, suggesting a possible role for sugars not only as carbon sinks but also as signaling molecules (Supplemental Note S1).

In this scenario, it is interesting to observe the presence of one carbohydrate intermediate more abundant in LL than ML, i.e. DHAP (LL versus ML = 1.97). Its accumulation is fully light-dependent in the framework of this experiment, as it is also more abundant in ML than in HL (ML/HL = 2.11; Fig. 7B). In plants, DHAP synthesis in the chloroplast is generally activated by light and acts as a precursor of starch biosynthesis. Even if this results should be taken with some caution, considering that DHAP was shown to have a rapid turnover (Arrivault et al., 2009; Mettler et al., 2014), this observation suggests an intriguing idea that DHAP could represent a checkpoint for metabolic reprogramming toward lipid biosynthesis instead of chrysolaminarin or laminarin biosynthesis.

Metabolic Regulation by Modulation of Intercellular Transport

Considering all data presented here, the subcellular compartmentalization of the enzymes producing/consuming DHAP and the trafficking of this triose phosphate from one compartment to another appear to be critical for carbon metabolic fluxes and carbon partitioning. In primary chloroplasts, DHAP is known to be

exported to the cytosol by the triose phosphate/phosphate translocator (TPT) in exchange for inorganic phosphate (Pi) needed to regenerate ATP in the stroma. In the secondary plastid of Apicomplexa (organisms presenting a plastid limited by four membranes, as in Eustigmatophyceae, but lacking photosynthesis), TPT translocators act in the opposite way, importing DHAP to feed the nonmevalonate pathway of isoprenoid synthesis and FA synthesis (Mullin et al., 2006; Brooks et al., 2010; Botté et al., 2012, 2013). We identified four genes coding for TPTs in *N. gaditana* (Naga_100100g11, Naga_101308g1, Naga_100006g37, and Naga_100007g104), and at least one of these genes has high homology with the Apicomplexa TPT (Naga_100100g11), showing conserved features such as 10 membrane-spanning domains and a chloroplastic transit peptide, suggesting a likely similar role in importing DHAP into the plastid. The presence of an Apicomplexa-like TPT suggests that *N. gaditana* might be able to import DHAP from the cytosol, possibly to feed IPP and FA syntheses. The four TPT genes of *N. gaditana* are down-regulated in HL, which could lead to decreased import of DHAP in the chloroplast under these conditions in favor of FA biosynthesis in the cytosol and in the ER. Although it still requires further experimental support, the hypothesis of a role of TPT translocators in regulation of metabolic fluxes in *Nannochloropsis* is consistent with all present data including the observed down-regulation of isoprenoids and FA within the plastid.

In an organism that grows phototrophically, such as *N. gaditana*, all reduced carbon molecules are first synthesized in the chloroplast and can be directly utilized there or exported to the cytosol.

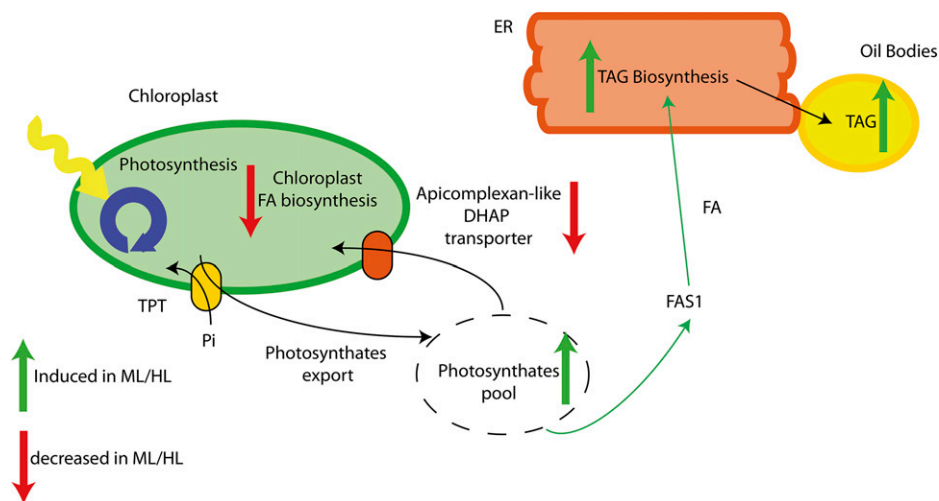


Figure 8. Model of regulation of carbon partitioning and lipid metabolisms in *N. gaditana* cells treated with high light. A possible mechanism for the modulation of lipid biosynthesis involving the triose phosphate/inorganic phosphate transporters is proposed. Pathways and metabolites that are down-/up-regulated in ML/HL are shown in red/green, respectively. In ML/HL, chloroplast FA biosynthesis is inhibited. Photosynthates exported to the cytoplasm might be converted into FA by a putative cytosolic FAS1. Based on the presented data, triose phosphate/inorganic phosphate transporters could be part of a regulatory loop controlling the carbon fluxes between the chloroplast and cytosol, determining a novel cellular metabolic status adapted to light intensity.

This study hypothesizes that the adaptation to high light involves a strong reorganization of the roles of the different organelles and supports a scenario where reduced carbon molecules can be transported back to the chloroplast to fuel plastid biosynthetic pathways such as isoprenoids and FA biosynthesis, initially fed on plastid precursors. Following this hypothesis, a regulatory loop for carbon partitioning between the chloroplast and cytosol could be tuned by modulating the activity of specific transporters. The regulation of metabolite fluxes in and out of the chloroplast could thus represent a major mechanism in the metabolic remodeling of the whole cell, increasing cytosolic pathways when needed (Fig. 8). Such a regulation, together with the peculiar *N. gaditana* ability of synthesizing FA in the cytosol, allows this algae to sustain a strong lipids biosynthesis in ER also in stressing conditions where the chloroplast pathway is repressed.

MATERIALS AND METHODS

Culture Conditions, Growth, and Neutral Lipid Content Determination

Nannochloropsis gaditana wild type from CCAP (Culture Collection of Algae and Protozoa), strain 849/5, was cultivated in sterile f/2 medium (Guillard and Ryther, 1962), using 32 g/L sea salts (S9883; Sigma-Aldrich), 40 mM Tris-HCl, pH 8, and Guillard's (f/2) marine water enrichment solution (G9903; Sigma-Aldrich). Cultures were generally kept in Erlenmeyer flasks with magnetic stirring or in plates on the same f/2 medium supplemented by agar 10 g/L, under continuous light at 100 $\mu\text{mol photons m}^{-2} \text{s}^{-1}$ at 21°C.

Before starting the experiment, cultures were treated with an antibiotic cocktail of Ampicillin (100 $\mu\text{g/mL}$), Streptomycin sulfate (100 $\mu\text{g/mL}$), and kanamycin sulfate (100 $\mu\text{g/mL}$; all from Sigma-Aldrich) for 48 h to obtain axenic cultures.

N. gaditana cells were precultured in a Drechsel bottle insufflated by 5% CO_2 (used both for mixing and providing the carbon source) for 2 weeks and diluted with new fresh f/2 medium every other day in order to keep the algae in exponential growth phase and restore the initial cellular concentration (20×10^6 cells/mL). The light intensity was set at 100 $\mu\text{mol photons m}^{-2} \text{s}^{-1}$ using daylight fluorescent lamps.

The same *N. gaditana* preculture in exponential growth phase and with a starting cellular concentration of 60×10^6 cells/mL was used to inoculate a Multi-Cultivator MC 1000-OD device (Photon Systems Instruments), at the constant temperature of 21°C, to generate the material for physiological, transcriptomic, metabolomic, and lipidomic analysis. The volume per tube was 80 mL, the starting OD_{720} was about 0.2, an air pump was used to aerate the culture and keep the cells in suspension, and then OD_{720} was measured every hour. After 5 d of acclimation, the algae growth was measured using a cell counter (Cellometer Auto X4; Nexcelom Bioscience). The biomass concentration was measured gravimetrically as a dry weight by filtering 5 mL of culture, diluted 1:5 with deionized water, using 0.45- μm pore size cellulose acetate filters. The filters were thus dried at 70°C for at least 24 h and the dry weight was expressed in grams per liter of culture.

The neutral lipid content was determined by staining the algal cell suspensions (2×10^6 cells in 1.9 mL final volume of deionized water) with Nile Red dye, 2.5 $\mu\text{g/mL}$ final concentration, for 10 min at 37°C. The fluorescence was measured using a spectrofluorimeter (OLIS DM45) with excitation wavelength at 488 nm and emission wavelength in the range of 500 and 700 nm. The relative fluorescence of Nile Red for the neutral lipids was obtained after the subtraction of the autofluorescence of algal cells and Nile Red alone.

Pigment Content Analysis and Chlorophyll Fluorescence Measurement

Total chlorophyll-a and carotenoids were extracted from the cells using 100% *N,N'*-dimethylformamide (Sigma-Aldrich), at 4°C, for at least 24 h. Pigment

concentration was determined spectrophotometrically using a Cary 100 spectrophotometer (Agilent Technologies). PSII maximum efficiency [expressed as $F_v/F_m = (F_m - F_0)/F_m$] was monitored through in vivo chlorophyll fluorescence determination with the DUAL-PAM-100 fluorimeter (Heinz-Walz). F_v/F_m under LL and ML conditions was consistent with the one reported for various *Nannochloropsis* species in other works (Kotabová et al., 2011; Simonato et al., 2011; Dong et al., 2013). PSII functional antenna size (ASII) was determined using a JTS10 spectrophotometer (Bio-Logic) at a concentration of 200×10^6 cells/mL, with 80 μM DCMU incubation for 10 min. In fluorescence induction kinetics, $t_{2/3}$ values were taken as the functional antenna size of PSII. Samples, for F_v/F_m and ASII determination were dark-adapted for 20 min before measuring (Perin et al., 2015).

Cultures Sampling for -Omics Data Collection

After 5 d of growth, independent photobioreactor tubes coming from the same biological run (thus representing technical replicates of growth) and exposed to the same light intensity were pulled together to get 20 mL for LL exposed cultures (2×10^7 cells/mL) and 10 mL for ML/HL exposed cultures (5 and 3.5×10^7 cells/mL, respectively). Cells were collected at 5,000g for 15 min at room temperature and then immediately frozen in liquid nitrogen. This procedure was followed for three independent photobioreactor runs in order to collect the biological material coming from three independent biological replicates.

RNA-Sequencing

RNA was extracted from frozen pellets using the RNeasy Plant Mini kit (Qiagen) and its quality checked with a bioanalyzer (Agilent Technologies). RNA was extracted from three independent biological replicates of *N. gaditana* cells grown for 5 d at three different light intensities. All the samples had an RNA integrity number of 7.2 to 7.8. Samples for ligation sequencing were prepared according to the SOLiD whole-transcriptome library preparation protocol (pn 4452437 Rev.B). Samples were sequenced using a SOLiD System 5500XL (Applied Biosystems). The average number of RNA-seq reads per sample was approximately 45 million and they ranged between 30 and 55 M (Supplemental Table S1). The reads of each of the nine samples (three biological replicates for each of the three light intensities) were mapped to the *N. gaditana* B-31 genome (Corteggiani Carpinelli et al., 2014) using PASS aligner (Campagna et al., 2013). The percentage identity was set to 90% with one gap allowed whereas the quality filtering parameters were set automatically by PASS. Moreover, a minimum read length cutoff of 50 and 30 nucleotides was set for the forward sequences and reverse reads, respectively. The spliced reads were identified using the procedure described in PASS manual (<http://pass.cribi.unipd.it>). Forward and reverse reads were aligned independently on the reference genome while the pairing between forward and reverse reads was performed using PASS-pair program from the PASS package. The abundance of each gene was quantified using htseq-counts program (<http://www-huber.embl.de/users/anders/HTSeq/doc/count.html>). The quantification was performed using only the uniquely mapped reads and providing as reference prediction the gene set available (Corteggiani Carpinelli et al., 2014).

Estimation of Differential Gene Expression

Differentially expressed gene analysis was performed using EdgeR software (Robinson et al., 2010). The raw read counts were normalized considering both the different depth of sequencing among the samples and the gene GC content. The normalization was performed using the EDASeq package (Risso et al., 2011). We considered as differentially expressed all the genes with a *P* value < 0.05 after false discovery rate correction.

Hierarchical Clustering

Cluster analysis of differentially expressed genes was performed using the TMEV 4.3 software (Significance Analysis of Microarray, multiclass analysis with 5% false discovery rate accepted; Saeed et al., 2003). Hierarchical clustering was performed on each cluster to represent gene relationships in dendrograms, with Pearson's correlation distance as the metric. Classes considered for clustering the differentially expressed genes were (1) cells grown in LL conditions, (2) cells grown in ML conditions, and (3) cells grown in HL conditions (three samples per each class). Gene Ontology analysis of the differentially expressed genes was performed according to Blast2GO web tool (Conesa et al., 2005).

Phylogenetic Analysis

Protein sequences were chosen among LHCA/b of *Chlamydomonas reinhardtii* and *Arabidopsis* (*Arabidopsis thaliana*), LHCf, mainly devoted to light harvesting and LHCX/LHCSR, involved in photoprotection. The multiple alignment of protein sequences was performed using MUSCLE (Edgar, 2004) and manually adjusted in BioEdit (Supplemental Fig. S1). Phylogeny reconstruction was performed using maximum likelihood as statistical method and 1000-iteration bootstrap resampling using Mega6.0 (Tamura et al., 2013). Results were also confirmed by performing a maximum likelihood analysis using PhyML (Guindon et al., 2010) and neighbor joining using Mega6.0 (Tamura et al., 2013).

Metabolomic Analysis

Liquid chromatography-positive electrospray ionization-mass spectrometry [LC-ESI(+)-MS] analysis of primary and secondary semipolar metabolome has been performed as previously described (De Vos et al., 2007; Iijima et al., 2008), with slight modifications. Metabolites were extracted from three independent biological replicates of *N. gaditana* cells grown for 5 d at three different light intensities. Ten milligrams of freeze-dried cells were extracted with 0.5 mL cold 75% (v/v) methanol and 0.1% (v/v) formic acid, spiked with 10 µg/mL formononetin. After grinding and sonication, the extracts have been shaken for 40' at 20 Hz using a Mixer Mill 300 (Qiagen) and centrifuged for 15' at 20,000g at 4°C. Supernatants (0.3 mL) were transferred to HPLC tubes.

For each sample, at least two independent extractions from the three independent cell cultures (for each light condition) were performed.

LC-MS analyses were carried out using a LTQ-Orbitrap Discovery mass spectrometry system (Thermo Fisher Scientific) operating in positive ESI, coupled to an Accela U-HPLC system (Thermo Fisher Scientific). Liquid chromatography was carried out using a Phenomenex C-18 Luna column (150 × 2.0 mm, 3 µm) and mobile phase was composed of water–0.1% formic acid (A) and acetonitrile–0.1% formic acid (B). The gradient was as follows: 95% A:5% B (1 min), a linear gradient to 25% A:75% B over 40 min, 2 min isocratic, before going back to the initial LC conditions in 18 min. Ten microliters of each sample was injected and a flow of 0.2 mL per minute was used during the whole LC runs. Detection was carried out continuously from 230 to 800 nm with an online Accela Surveyor photodiode array detector (Thermo Fisher Scientific). All solvents used were LC-MS grade quality (CHROMASOLV; Sigma-Aldrich).

Glycerolipid Analysis

Glycerolipids were extracted from three independent biological replicates of *N. gaditana* cells grown for 5 d at three different light intensities. Glycerolipids were extracted from 10 mg of freeze-dried *N. gaditana* cells, according to Folch et al. (1957). The freeze-dried cell pellet was resuspended in 4 mL of boiling ethanol for 5 min followed by the addition of 2 mL of methanol and 8 mL of chloroform at room temperature.

The mixture was then saturated with argon and stirred for 1 h at room temperature. After filtration through glass wool, cell remains were rinsed with 3 mL of chloroform/methanol, 2:1 (v/v). In order to initiate biphasic formation, 5 mL of 1% NaCl was then added to the filtrate. The chloroform phase was dried under argon before resolubilization of the lipid extract in pure chloroform.

To isolate TAGs, lipids were run on silica gel plates (Merck) with hexane: diethylether:acetic acid, 70:30:1 (v/v). To isolate polar glycerolipids, lipids were analyzed on silica gel plates (Merck) by two-dimensional thin-layer chromatography (2D-TLC). The first solvent was chloroform:methanol:water, 65:25:4 (v/v), while the second one was chloroform:acetone:methanol:acetic acid:water, 50:20:10:10:5 (v/v). Lipids were then visualized under UV light after pulverization of 8-anilino-1-naphthalenesulfonic acid at 2% in methanol. Lipid classes were then assessed based on position on the 2D-TLC, according to previous studies (Simionato et al., 2013), adding a DGTS standard that was not used in this previous study. Carboxymethyl phosphatidylethanolamine was identified by mass spectrometry as described by Shoji et al. (2010). Glycerolipids were then scraped off from the 2D-TLC plates for further analyses. For lipid quantification, fatty acids were methylated using 3 mL of 2.5% H₂SO₄ in methanol during 1 h at 100°C (including standard amounts of 21:0). The reaction was stopped by the addition of 3 mL of water and 3 mL of hexane. The hexane phase was analyzed by gas and liquid chromatography (Perkin-Elmer) on a BPX70 column (SGE Analytical Science), coupled with MS. Methylated fatty acids were identified by comparison of their retention times with those of standards and quantified by surface peak method using 21:0. For every biological replicate, the extraction and quantification were repeated at least for three technical replicates.

Large Data Sets

Since the data sets we refer to are too large to be included in the manuscript, they are uploaded as supplemental material.

Accession Numbers

Sequence data used for phylogenetic reconstruction can be found in the GenBank data library under the following accession numbers: AtLhca2, AT3G61470; AtLhca3, AT1G61520; AtLhca4, AT3G47470; AtLhcb1.1, AT1G29930; AtLhcb2.1, AT2G05070; AtLhcb5, AT4G10340; CrLhca3, XP_001701405; CrLhca4, XP_001698519; CrLhcb5, XP_001695927; CrLhcbm2, XP_001700243; CrLhcbm2, XP_001694115; CeLHCSR, X60721; SoLHCSR, DQ394297; MvLHCSR, DQ370082; OtLHCSR, AY954739; CrLHCSR3, XM_001696073; CrLHCSR1, XM_001696086; PpLHCSR1, XM_001776900; PpLHCSR2, XM_001768019; TpLHCX6, XM_002295147; EsiLHCX1, CBJ48499; EsiLHCX2, CBN73961; EsiLHCX3, CBJ27268; EsiLHCx4, CBJ27787; EsiLHCX5, CBJ27788; EsiLHCX6, CBJ27803; EsiLHCX7, CBJ27803; NgLhcx1, EWM30071; NgLHCf1, EWM21572.1; NgLHCX2, EWM27041; PtlLHCf12, XM_002176699; TpLHCf7, XM_002294544; PtlLHCf11, XM_002184727; PtlLHCf10, XM_002183345; TpLHCf10, XM_002295583; EsiLHCf1, CBN76797; EsiLHCf2, CBN74050; EsiLHCf3, CBJ30555; EsiLHCf4, CBN76797; PtlLHCf13, XP_002182219; PtlLHCf14, XP_002182305; CycLHCf1, CAA04178; TpLHCf1, XP_002294743; TpLHCf3, XP_002295015; TpLHCf4, XP_002294845; TpLHCf5, XP_002294608; TpLHCf6, XP_002288729; TpLHCf8, XP_002286436.

Supplemental Material

The following supplemental materials are available.

Supplemental Figure S1. Protein sequence analysis of a subset of LHC sequences from algae, *Physcomitrella patens*, and *Arabidopsis thaliana*.

Supplemental Figure S2. Light effect on the growth of *Nannochloropsis gaditana* cells.

Supplemental Figure S3. Two dimensional MDS plot for the light transcriptome data set.

Supplemental Figure S4. Distribution of genes in manual functional categories for the six groups identified by hierarchical clustering analysis.

Supplemental Table S1. Description of the SOLID whole-transcriptome RNA-seq libraries.

Supplemental Table S2. Nonpolar metabolites in *Nannochloropsis gaditana* cells grown in three different light conditions.

Supplemental Note S1. Genes clusters description according to Gene Ontology annotation.

Supplemental Note S2. Effect of light on various metabolic pathways.

Supplemental Note S3. Effect of light on desaturases behavior.

Supplemental Methods S1. Isoprenoid determination.

Supplemental Data Set S1. Light dose-regulated genes in *Nannochloropsis gaditana*.

Supplemental Data Set S2. Light response of various group of genes related to plastid physiology and metabolism in *Nannochloropsis gaditana*.

Supplemental Data Set S3. Light response of various groups of genes involved in primary carbon and lipid metabolism in *Nannochloropsis gaditana*.

Supplemental Data Set S4. LC-ESI-MS of semipolar metabolites in *Nannochloropsis gaditana* cells grown in three different light conditions.

ACKNOWLEDGMENTS

We thank Gino Schiano di Visconte for helping in the setup of the conditions of LC-MS for metabolomics analyses.

Received April 14, 2016; accepted June 20, 2016; published June 20, 2016.

LITERATURE CITED

- Abida H, Dolch L-J, Meï C, Villanova V, Conte M, Block MA, Finazzi G, Bastien O, Tirichine L, Bowler C, et al (2015) Membrane glycerolipid remodeling triggered by nitrogen and phosphorus starvation in *Phaeodactylum tricornutum*. *Plant Physiol* **167**: 118–136
- Alboresi A, Gerotto C, Giacometti GM, Bassi R, Morosinotto T (2010) *Physcomitrella patens* mutants affected on heat dissipation clarify the evolution of photoprotection mechanisms upon land colonization. *Proc Natl Acad Sci USA* **107**: 11128–11133
- Arrivault S, Guenther M, Ivakov A, Feil R, Vosloh D, van Dongen JT, Sulpice R, Stitt M (2009) Use of reverse-phase liquid chromatography, linked to tandem mass spectrometry, to profile the Calvin cycle and other metabolic intermediates in *Arabidopsis* rosettes at different carbon dioxide concentrations. *Plant J* **59**: 826–839
- Bailey S, Walters RG, Jansson S, Horton P (2001) Acclimation of *Arabidopsis thaliana* to the light environment: the existence of separate low light and high light responses. *Planta* **213**: 794–801
- Beer A, Gundermann K, Beckmann J, Büchel C (2006) Subunit composition and pigmentation of fucoxanthin-chlorophyll proteins in diatoms: evidence for a subunit involved in diadinoxanthin and diatoxanthin binding. *Biochemistry* **45**: 13046–13053
- Blaby IK, Glaesener AG, Mettler T, Fitz-Gibbon ST, Gallaher SD, Liu B, Boyle NR, Kropat J, Stitt M, Johnson S, et al (2013) Systems-level analysis of nitrogen starvation-induced modifications of carbon metabolism in a *Chlamydomonas reinhardtii* starchless mutant. *Plant Cell* **25**: 4305–4323
- Bogen C, Al-Dilaimi A, Albersmeier A, Wichmann J, Grundmann M, Rupp O, Lauersen KJ, Blifernez-Klassen O, Kalinowski J, Goemann A, Mussnug JH, Kruse O (2013) Reconstruction of the lipid metabolism for the microalga *Monoraphidium neglectum* from its genome sequence reveals characteristics suitable for biofuel production. *BMC Genomics* **14**: 926
- Botté CY, Dubar F, McFadden GI, Maréchal E, Biot C (2012) Plasmodium falciparum apicoplast drugs: targets or off-targets? *Chem Rev* **112**: 1269–1283
- Botté CY, Yamaro-Botté Y, Rupasinghe TWT, Mullin KA, MacRae JI, Spurck TP, Kalanon M, Shears MJ, Coppel RL, Crellin PK, et al (2013) Atypical lipid composition in the purified relic plastid (apicoplast) of malaria parasites. *Proc Natl Acad Sci USA* **110**: 7506–7511
- Boussiba S, Vonshak A, Cohen Z, Avissar Y, Richmond A (1987) Lipid and biomass production by the halotolerant microalga *Nannochloropsis salina*. *Biomass* **12**: 37–47
- Brooks CF, Johnsen H, van Dooren GG, Muthalagi M, Lin SS, Bohne W, Fischer K, Striepen B (2010) The toxoplasma apicoplast phosphate translocator links cytosolic and apicoplast metabolism and is essential for parasite survival. *Cell Host Microbe* **7**: 62–73
- Campagna D, Telatin A, Forcato C, Vitulo N, Valle G (2013) PASS-bis: a bisulfite aligner suitable for whole methylome analysis of Illumina and SOLiD reads. *Bioinformatics* **29**: 268–270
- Chen M, Thelen JJ (2010) The plastid isoform of triose phosphate isomerase is required for the postgerminative transition from heterotrophic to autotrophic growth in *Arabidopsis*. *Plant Cell* **22**: 77–90
- Conesa A, Götz S, García-Gómez JM, Terol J, Talón M, Robles M (2005) Blast2GO: a universal tool for annotation, visualization and analysis in functional genomics research. *Bioinformatics* **21**: 3674–3676
- Contento AL, Kim S-J, Bassham DC (2004) Transcriptome profiling of the response of *Arabidopsis* suspension culture cells to Suc starvation. *Plant Physiol* **135**: 2330–2347
- Corteggiani Carpinelli E, Telatin A, Vitulo N, Forcato C, D'Angelo M, Schiavon R, Vezzi A, Giacometti GM, Morosinotto T, Valle G (2014) Chromosome scale genome assembly and transcriptome profiling of *Nannochloropsis gaditana* in nitrogen depletion. *Mol Plant* **7**: 323–335
- Couée I, Sulmon C, Gouesbet G, El Amrani A (2006) Involvement of soluble sugars in reactive oxygen species balance and responses to oxidative stress in plants. *J Exp Bot* **57**: 449–459
- De Martino A, Douady D, Quinet-Szely M, Rousseau B, Crépineau F, Apt K, Caron L (2000) The light-harvesting antenna of brown algae: highly homologous proteins encoded by a multigene family. *Eur J Biochem* **267**: 5540–5549
- Dietz K-J (2015) Efficient high light acclimation involves rapid processes at multiple mechanistic levels. *J Exp Bot* **66**: 2401–2414
- Dong H-P, Williams E, Wang DZ, Xie Z-X, Hsia RC, Jenck A, Halden R, Li J, Chen F, Place AR (2013) Responses of *Nannochloropsis oceanica* IMET1 to long-term nitrogen starvation and recovery. *Plant Physiol* **162**: 1110–1126
- Edgar RC (2004) MUSCLE: multiple sequence alignment with high accuracy and high throughput. *Nucleic Acids Res* **32**: 1792–1797
- Elbein AD, Pan YT, Pastuszak I, Carroll D (2003) New insights on trehalose: a multifunctional molecule. *Glycobiology* **13**: 17R–27R
- Endo K, Mizusawa N, Shen J-R, Yamada M, Tomo T, Komatsu H, Kobayashi M, Kobayashi K, Wada H (2015) Site-directed mutagenesis of amino acid residues of D1 protein interacting with phosphatidylglycerol affects the function of plastoquinone QB in photosystem II. *Photosynth Res* **126**: 385–397
- Falkowski PG, Katz ME, Knoll AH, Quigg A, Raven JA, Schofield O, Taylor FJR (2004) The evolution of modern eukaryotic phytoplankton. *Science* **305**: 354–360
- Folch J, Lees M, Sloane Stanley GH (1957) A simple method for the isolation and purification of total lipides from animal tissues. *J Biol Chem* **226**: 497–509
- Guillard RR, Ryther JH (1962) Studies of marine planktonic diatoms. I. *Cyclotella nana* Hustedt, and *Detonula confervacea* (Cleve) Gran. *Can J Microbiol* **8**: 229–239
- Guindon S, Dufayard J-F, Lefort V, Anisimova M, Hordijk W, Gascuel O (2010) New algorithms and methods to estimate maximum-likelihood phylogenies: assessing the performance of PhyML 3.0. *Syst Biol* **59**: 307–321
- Ho S-H, Chan M-C, Liu C-C, Chen C-Y, Lee W-L, Lee D-J, Chang J-S (2014) Enhancing lutein productivity of an indigenous microalga *Scenedesmus obliquus* FSP-3 using light-related strategies. *Bioresour Technol* **152**: 275–282
- Hu Q, Sommerfeld M, Jarvis E, Ghirardi M, Posewitz M, Seibert M, Darzins A (2008) Microalgal triacylglycerols as feedstocks for biofuel production: perspectives and advances. *Plant J* **54**: 621–639
- Iijima Y, Nakamura Y, Ogata Y, Tanaka K, Sakurai N, Suda K, Suzuki T, Suzuki H, Okazaki K, Kitayama M, et al (2008) Metabolite annotations based on the integration of mass spectral information. *Plant J* **54**: 949–962
- Ikeda Y, Yamagishi A, Komura M, Suzuki T, Dohmae N, Shibata Y, Itoh S, Koike H, Satoh K (2013) Two types of fucoxanthin-chlorophyll-binding proteins I tightly bound to the photosystem I core complex in marine centric diatoms. *Biochim Biophys Acta* **1827**: 529–539
- Jia J, Han D, Gerken HG, Li Y, Sommerfeld M, Hu Q, Xu J (2015) Molecular mechanisms for photosynthetic carbon partitioning into storage neutral lipids in *Nannochloropsis oceanica* under nitrogen-depletion conditions. *Algal Res* **7**: 66–77
- Johnson X, Alric J (2013) Central carbon metabolism and electron transport in *Chlamydomonas reinhardtii*: metabolic constraints for carbon partitioning between oil and starch. *Eukaryot Cell* **12**: 776–793
- Kotabová E, Kaňa R, Jarešová J, Prášil O (2011) Non-photochemical fluorescence quenching in *Chromera velia* is enabled by fast violaxanthin de-epoxidation. *FEBS Lett* **585**: 1941–1945
- Lepetit B, Volke D, Szabó M, Hoffmann R, Garab G, Wilhelm C, Goss R (2007) Spectroscopic and molecular characterization of the oligomeric antenna of the diatom *Phaeodactylum tricornutum*. *Biochemistry* **46**: 9813–9822
- Li J, Han D, Wang D, Ning K, Jia J, Wei L, Jing X, Huang S, Chen J, Li Y, Hu Q, Xu J (2014) Choreography of transcriptomes and lipidomes of *Nannochloropsis* reveals the mechanisms of oil synthesis in microalgae. *Plant Cell* **26**: 1645–1665
- Lu Y, Tarkowská D, Turečková V, Luo T, Xin Y, Li J, Wang Q, Jiao N, Strnad M, Xu J (2014) Antagonistic roles of abscisic acid and cytokinin during response to nitrogen depletion in oleaginous microalga *Nannochloropsis oceanica* expand the evolutionary breadth of phytohormone function. *Plant J* **80**: 52–68
- Lunn JE, Delorge I, Figueroa CM, Van Dijck P, Stitt M (2014) Trehalose metabolism in plants. *Plant J* **79**: 544–567
- Martin GJO, Hill DRA, Olmstead ILD, Bergamin A, Shears MJ, Dias DA, Kentish SE, Scales PJ, Botté CY, Callahan DL (2014) Lipid profile remodeling in response to nitrogen deprivation in the microalgae *Chlorella* sp. (Trebouxiophyceae) and *Nannochloropsis* sp. (Eustigmatophyceae). *PLoS One* **9**: e103389
- Maxwell DP, Falk S, Trick CG, Huner N (1994) Growth at low temperature mimics high-light acclimation in *Chlorella vulgaris*. *Plant Physiol* **105**: 535–543

- Meng Y, Jiang J, Wang H, Cao X, Xue S, Yang Q, Wang W (2015) The characteristics of TAG and EPA accumulation in *Nannochloropsis oceanica* IMET1 under different nitrogen supply regimes. *Bioresour Technol* **179**: 483–489
- Mettler T, Mühlhaus T, Hemme D, Schöttler M-A, Rupprecht J, Idoine A, Veyel D, Pal SK, Yaneva-Roder L, Winck FV, et al (2014) Systems analysis of the response of photosynthesis, metabolism, and growth to an increase in irradiance in the photosynthetic model organism *Chlamydomonas reinhardtii*. *Plant Cell* **26**: 2310–2350
- Miller R, Wu G, Deshpande RR, Vieler A, Gärtner K, Li X, Moellering ER, Zäuner S, Cornish AJ, Liu B, et al (2010) Changes in transcript abundance in *Chlamydomonas reinhardtii* following nitrogen deprivation predict diversion of metabolism. *Plant Physiol* **154**: 1737–1752
- Mullin KA, Lim L, Ralph SA, Spurck TP, Handman E, McFadden GI (2006) Membrane transporters in the relict plastid of malaria parasites. *Proc Natl Acad Sci USA* **103**: 9572–9577
- Pal D, Khozin-Goldberg I, Cohen Z, Boussiba S (2011) The effect of light, salinity, and nitrogen availability on lipid production by *Nannochloropsis* sp. *Appl Microbiol Biotechnol* **90**: 1429–1441
- Peers G, Truong TB, Ostendorf E, Busch A, Elrad D, Grossman AR, Hippler M, Niyogi KK (2009) An ancient light-harvesting protein is critical for the regulation of algal photosynthesis. *Nature* **462**: 518–521
- Pego JV, Kortstee AJ, Huijser C, Smeekens SC (2000) Photosynthesis, sugars and the regulation of gene expression. *J Exp Bot* **51**: 407–416
- Perin G, Bellan A, Segalla A, Meneghesso A, Alboresi A, Morosinotto T (2015) Generation of random mutants to improve light-use efficiency of *Nannochloropsis gaditana* cultures for biofuel production. *Biotechnol Biofuels* **8**: 161
- Petroutsos D, Amiar S, Abida H, Dolch L-J, Bastien O, Rébeillé F, Jouhet J, Falconet D, Block MA, McFadden GI, et al (2014) Evolution of galactoglycerolipid biosynthetic pathways—from cyanobacteria to primary plastids and from primary to secondary plastids. *Prog Lipid Res* **54**: 68–85
- Poliner E, Panchy N, Newton L, Wu G, Lapinsky A, Bullard B, Zienkiewicz A, Benning C, Shiu S-H, Farré EM (2015) Transcriptional coordination of physiological responses in *Nannochloropsis oceanica* CCMP1779 under light/dark cycles. *Plant J* **83**: 1097–1113
- Radakovits R, Jinkerson RE, Darzins A, Posewitz MC (2010) Genetic engineering of algae for enhanced biofuel production. *Eukaryot Cell* **9**: 486–501
- Ramakrishnan S, Serricchio M, Striepen B, Büttikofer P (2013) Lipid synthesis in protozoan parasites: a comparison between kinetoplastids and apicomplexans. *Prog Lipid Res* **52**: 488–512
- Richard C, Ouellet H, Guertin M (2000) Characterization of the LI818 polypeptide from the green unicellular alga *Chlamydomonas reinhardtii*. *Plant Mol Biol* **42**: 303–316
- Risso D, Schwartz K, Sherlock G, Dudoit S (2011) GC-content normalization for RNA-Seq data. *BMC Bioinformatics* **12**: 480
- Robinson MD, McCarthy DJ, Smyth GK (2010) edgeR: a Bioconductor package for differential expression analysis of digital gene expression data. *Bioinformatics* **26**: 139–140
- Rodolfi L, Chini Zittelli G, Bassi N, Padovani G, Biondi N, Bonini G, Tredici MR (2009) Microalgae for oil: strain selection, induction of lipid synthesis and outdoor mass cultivation in a low-cost photobioreactor. *Biotechnol Bioeng* **102**: 100–112
- Rolland F, Baena-Gonzalez E, Sheen J (2006) Sugar sensing and signaling in plants: conserved and novel mechanisms. *Annu Rev Plant Biol* **57**: 675–709
- Ryu J-Y, Song JY, Lee JM, Jeong SW, Chow WS, Choi S-B, Pogson BJ, Park Y-I (2004) Glucose-induced expression of carotenoid biosynthesis genes in the dark is mediated by cytosolic pH in the cyanobacterium *Synechocystis* sp. PCC 6803. *J Biol Chem* **279**: 25320–25325
- Saeed AI, Sharov V, White J, Li J, Liang W, Bhagabati N, Braisted J, Klapa M, Currier T, Thiagarajan M, et al (2003) TM4: a free, open-source system for microarray data management and analysis. *Biotechniques* **34**: 374–378
- Sforza E, Simionato D, Giacometti GM, Bertuccio A, Morosinotto T (2012) Adjusted light and dark cycles can optimize photosynthetic efficiency in algae growing in photobioreactors. *PLoS One* **7**: e38975
- Shoji N, Nakagawa K, Asai A, Fujita I, Hashiura A, Nakajima Y, Oikawa S, Miyazawa T (2010) LC-MS/MS analysis of carboxymethylated and carboxyethylated phosphatidylethanolamines in human erythrocytes and blood plasma. *J Lipid Res* **51**: 2445–2453
- Simionato D, Block MA, La Rocca N, Jouhet J, Maréchal E, Finazzi G, Morosinotto T (2013) The response of *Nannochloropsis gaditana* to nitrogen starvation includes de novo biosynthesis of triacylglycerols, a decrease of chloroplast galactolipids, and reorganization of the photosynthetic apparatus. *Eukaryot Cell* **12**: 665–676
- Simionato D, Sforza E, Corteggiani Carpinelli E, Bertuccio A, Giacometti GM, Morosinotto T (2011) Acclimation of *Nannochloropsis gaditana* to different illumination regimes: effects on lipids accumulation. *Bioresour Technol* **102**: 6026–6032
- Slocome SP, Zhang Q, Ross M, Anderson A, Thomas NJ, Lapresa Á, Rad-Menéndez C, Campbell CN, Black KD, Stanley MS, Day JG (2015) Unlocking nature's treasure-chest: screening for oleaginous algae. *Sci Rep* **5**: 9844
- Stitt M, Zeeman SC (2012) Starch turnover: pathways, regulation and role in growth. *Curr Opin Plant Biol* **15**: 282–292
- Stoop J, Williamson J, Masonpharr D (1996) Mannitol metabolism in plants: a method for coping with stress. *Trends Plant Sci* **1**: 139–144
- Tamura K, Stecher G, Peterson D, Filipowski A, Kumar S (2013) MEGA6: Molecular Evolutionary Genetics Analysis version 6.0. *Mol Biol Evol* **30**: 2725–2729
- Tanaka T, Maeda Y, Veluchamy A, Tanaka M, Abida H, Maréchal E, Bowler C, Muto M, Sunaga Y, Tanaka M, et al (2015) Oil accumulation by the oleaginous diatom *Fistulifera solaris* as revealed by the genome and transcriptome. *Plant Cell* **27**: 162–176
- Teo CL, Idris A, Zain NAM, Taisir M (2014) Synergistic effect of optimizing light-emitting diode illumination quality and intensity to manipulate composition of fatty acid methyl esters from *Nannochloropsis* sp. *Bioresour Technol* **173**: 284–290
- Vieler A, Wu G, Tsai C-H, Bullard B, Cornish AJ, Harvey C, Reza I-B, Thornburg C, Achawanantakun R, Buehl CJ, et al (2012) Genome, functional gene annotation, and nuclear transformation of the heterokont oleaginous alga *Nannochloropsis oceanica* CCMP1779. *PLoS Genet* **8**: e1003064
- Vítová M, Bišová K, Kawano S, Zachleder V (2015) Accumulation of energy reserves in algae: From cell cycles to biotechnological applications. *Biotechnol Adv* **33**: 1204–1218
- De Vos RCH, Moco S, Lommen A, Keurentjes JJB, Bino RJ, Hall RD (2007) Untargeted large-scale plant metabolomics using liquid chromatography coupled to mass spectrometry. *Nat Protoc* **2**: 778–791
- Wang D, Ning K, Li J, Hu J, Han D, Wang H, Zeng X, Jing X, Zhou Q, Su X, et al (2014) *Nannochloropsis* genomes reveal evolution of microalgal oleaginous traits. *PLoS Genet* **10**: e1004094
- Wang Y, Duanmu D, Spalding MH (2011) Carbon dioxide concentrating mechanism in *Chlamydomonas reinhardtii*: inorganic carbon transport and CO₂ recapture. *Photosynth Res* **109**: 115–122
- Zaffagnini M, Michelet L, Sciabolini C, Di Giacinto N, Morisse S, Marchand CH, Trost P, Fermani S, Lemaire SD (2014) High-resolution crystal structure and redox properties of chloroplastic triosephosphate isomerase from *Chlamydomonas reinhardtii*. *Mol Plant* **7**: 101–120
- Zhao B, Su Y (2014) Process effect of microalgal-carbon dioxide fixation and biomass production: A review. *Renew Sustain Energy Rev* **31**: 121–132
- Zhu S-H, Green BR (2010) Photoprotection in the diatom *Thalassiosira pseudonana*: role of LI818-like proteins in response to high light stress. *Biochim Biophys Acta* **1797**: 1449–1457